Analysis of Plasma Distribution near the Extraction Region in Negative Ion Sources with Surface and Volume Produced Negative Ions*)

Azusa FUKANO and Akiyoshi HATAYAMA[1)]

Monozukuri Department, Tokyo Metropolitan College of Industrial Technology, Higashi-Oi, Shinagawa, Tokyo 140-0011, Japan

[1)]*Faculty of Science and Technology, Keio University, Hiyoshi, Kohoku-ku, Yokohama, Kanagawa 223-8522, Japan*

(Received 18 December 2018 / Accepted 9 April 2019)

Plasma distributions near the extraction region in a hydrogen negative ion source are investigated analytically. Where surface produced hydrogen negative ions and volume produced hydrogen negative ions are considered in addition to electrons and hydrogen positive ions. The plasma-sheath equation is derived analytically and the distributions of the electric potential and the plasma density near the extraction region are obtained by solving the plasma-sheath equation. It is shown that the region consisting of the positive ions and the negative ions more than the electrons is formed near the extraction region for a case of large production rate of the negative ions. Dependence of the plasma density on the temperature of the negative ions is also shown.

Keywords: negative ion source, volume produced negative ion, surface produced negative ion, plasma-sheath equation, electric potential, plasma density

DOI: 10.1585/pfr.14.3403096

1. Introduction

Neutral beam injection (NBI) using a hydrogen negative ion source is one of the most promising method of heating plasma confined magnetically. In the hydrogen negative ion source, it is important to understand the plasma characteristics near the extraction region in order to extract a large amount of hydrogen negative ions. The emission of electrons from a cathode into the sheath in plasma containing positive ions, electrons and negative ions has been analyzed by Amemiya *et al.* [1]. For the case of the emission of negative ions from the cathode into the sheath, transport of surface produced negative ions from a cathode has been analyzed by McAdams and Bacal [2]. Their results are in good agreement with the 1D3 V PIC code [3]. Formation of a plasma well has been also shown by one-dimensional analytical model of the sheath in the negative ion source [4]. The plasma well and the particle density in the negative ion source have been studied and confirmed also by 2D PIC model simulations [5,6]. On the other hand, an experiment in the NIFS-R&D ion source has suggested that a "double ion plasma layer" which is a region consisting of mainly hydrogen positive ions (H^+) and negative ions (H^-) exists near a plasma grid (PG) surface [7]. The distribution of the plasma density near the wall is related to the electric potential distribution. Emmert *et al.* have investigated formation of the potential by using a plasma-sheath equation for plasma consisting of positive ions and electrons [8]. The distribution of the plasma density near the extraction region in a surface produced negative ion source has been studied analytically and it has been shown that as the production rate of the surface produced H^- ions increases the double ion plasma layer is formed near the PG surface [9]. However the effect of the volume produced H^- ions has not been considered.

In this paper, we will study the distributions of the electric potential and the plasma density near the extraction region in the hydrogen negative ion sources, where surface produced H^- ions and volume produced H^- ions are considered in addition to electrons and H^+ ions. The plasma-sheath equation is derived analytically and the distributions of the electric potential and the plasma density are obtained. Effect of the production rate and the temperature of the H^- ions on the plasma distribution near the extraction region are shown.

2. Analysis of Electric Potential

2.1 Analytical model and basic equations

The geometry of the extraction region in the model is shown in Fig. 1. It is assumed that in the hydrogen negative ion source the surface produced H^- ions are produced on the PG surface and launched to the interior of the ion source and the volume produced H^- ions and the H^+ ions are produced whole in the ion source. The problem is treated as one-dimensional model in x-direction, which is the direction of beam extraction. In the analysis, the PG is

author's e-mail: fukano@metro-cit.ac.jp

*) This article is based on the presentation at the 27th International Toki Conference (ITC27) & the 13th Asia Pacific Plasma Theory Conference (APPTC2018).

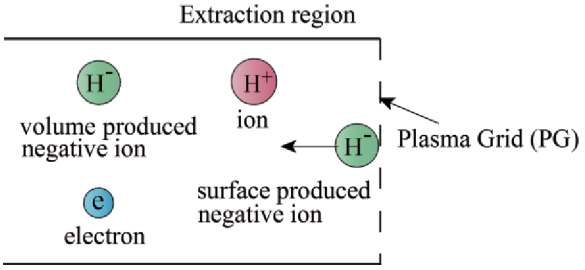

Fig. 1 Geometry of the extraction region of the model.

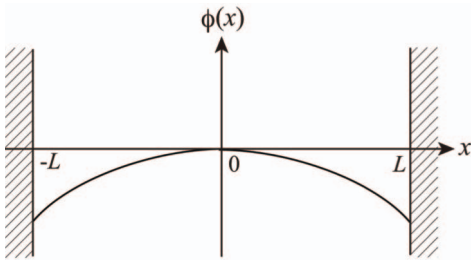

Fig. 2 Geometry of the potential in the analytical model.

considered to be the walls on both sides in order to maintain a conservation of particles. It is assumed that the electric potential $\phi(x)$ is symmetric about $x = 0$ and decreases toward the walls and is zero at $x = 0$ as shown in Fig. 2. The walls at $x = \pm L$ are assumed to be perfectly absorbing and electrically floating. The total energy E_i of the H^+ ion, E_v of the volume produced H^- ion, and E_s of the surface produced H^- ion in the x-direction are

$$E_i = \frac{1}{2}M_i v_i^2 + q\phi(x), \tag{1}$$

$$E_v = \frac{1}{2}M_v v_v^2 - q\phi(x), \tag{2}$$

$$E_s = \frac{1}{2}M_s v_s^2 - q\phi(x), \tag{3}$$

where M_i, M_v, and M_s are the masses, υ_i, υ_v, and υ_s are the velocities, q and $-q$ are the charges of the H^+ ion and the H^- ion, respectively. The subscripts "i", "v", and "s" denote value belonging to the H^+ ion, the volume produced H^- ion, and the surface produced H^- ion, respectively throughout this paper. The kinetic equations for the H^+ ion and the H^- ion in the phase space (x, E_i), (x, E_v), and (x, E_s) are described by

$$\sigma v_i(x, E_i)\frac{\partial f_i(x, E_i, \sigma)}{\partial x} = S_i(x, E_i), \tag{4}$$

$$\sigma v_v(x, E_v)\frac{\partial f_v(x, E_v, \sigma)}{\partial x} = S_v(x, E_v), \tag{5}$$

$$\sigma v_s(x, E_s)\frac{\partial f_s(x, E_s, \sigma)}{\partial x} = S_s(x, E_s), \tag{6}$$

where $\sigma = \pm 1$ is the direction of the particle motion, $f_i(x, E_i, \sigma)$, $f_v(x, E_v, \sigma)$, and $f_s(x, E_s, \sigma)$ are the distribution functions, and $S_i(x, E_i)$, $S_v(x, E_v)$, and $S_s(x, E_s)$ are the source functions. We assume a symmetry about $x = 0$ for the source functions. Furthermore, we assume that particles are not reflected at the walls, then the boundary conditions of the distribution functions are $f_i(-L, E_i, +1) = f_i(L, E_i, -1) = 0$, $f_v(-L, E_v, +1) = f_v(L, E_v, -1) = 0$, and $f_s(-L, E_s, +1) = f_s(L, E_s, -1) = 0$.

2.2 Plasma-sheath equation

From Eqs. (1), (2), and (3), the ion velocities are given by $\upsilon_i = [(2/M_i)\{E_i - q\phi(x)\}]^{1/2}$, $\upsilon_v = [(2/M_v)\{E_v + q\phi(x)\}]^{1/2}$, and $\upsilon_s = [(2/M_s)\{E_s + q\phi(x)\}]^{1/2}$. The energy space of the particle is divided to some regions, which is based on the condition that υ_i, υ_v, and υ_s must be real number, that is, $E_i - q\phi(x) \geq 0$, $E_v + q\phi(x) \geq 0$, and $E_s + q\phi(x) \geq 0$, respectively. The particle motion depends on its energy. The distribution functions $f_i(x, E_i, \sigma)$, $f_v(x, E_v, \sigma)$, and $f_s(x, E_s, \sigma)$ for $\sigma = \pm 1$ are obtained by integrating Eqs. (4), (5), and (6) for particle trajectory with the boundary conditions. The ion densities are obtained by taking the sum of the distribution functions about $\sigma = \pm 1$ for each energy region and integrating them for E_i, E_v, and E_s, respectively, as

$$n_i(x) = \sum_\sigma \int dE_i \frac{f_i(x, E_i, \sigma)}{v_i(x, E_i)}, \tag{7}$$

$$n_v(x) = \sum_\sigma \int dE_v \frac{f_v(x, E_v, \sigma)}{v_v(x, E_v)}, \tag{8}$$

$$n_s(x) = \sum_\sigma \int dE_s \frac{f_s(x, E_s, \sigma)}{v_s(x, E_s)}, \tag{9}$$

where

$$\sum_\sigma f_i(x, E_i, \sigma) = \begin{cases} 2\displaystyle\int_0^L \frac{S_i(x_i', E_i)}{v_i(x_i', E_i)}dx_i', \\ \qquad (0 < E_i < \infty) \\ 2\displaystyle\int_{x_{it}}^L \frac{S_i(x_i', E_i)}{v_i(x_i', E_i)}dx_i', \\ \qquad (E_{min} < E_i < 0) \end{cases}, \tag{10}$$

$$\sum_\sigma f_v(x, E_v, \sigma) = \begin{cases} 2\displaystyle\int_0^L \frac{S_v(x_v', E_v)}{v_v(x_v', E_v)}dx_v', \\ \qquad (-q\phi_{min} < E_v < \infty) \\ 2\displaystyle\int_0^{x_{vt1}} \frac{S_v(x_v', E_v)}{v_v(x_v', E_v)}dx_v', \\ \qquad (E_{min-} < E_v < -q\phi_{min}) \\ 2\displaystyle\int_{x_{vt2}}^L \frac{S_v(x_v', E_v)}{v_v(x_v', E_v)}dx_v', \\ \qquad (-q\phi(\pm L) < E_v < -q\phi_{min}) \end{cases}, \tag{11}$$

$$\sum_\sigma f_s(x, E_s, \sigma) = \begin{cases} 2\displaystyle\int_0^L \frac{S_s(x_s', E_s)}{v_s(x_s', E_s)}dx_s', \\ \qquad (-q\phi_{min} < E_s < \infty) \\ 2\displaystyle\int_{x_{st}}^L \frac{S_s(x_s', E_s)}{v_s(x_s', E_s)}dx_s', \\ \qquad (E_{min-} < E_s < -q\phi_{min}) \end{cases}, \tag{12}$$

where x_i', x_v', and x_s' are the generation positions of the ions, x_{it} and x_{st} are the turning points of the H^+ ions and the

surface produced H^- ions, respectively, x_{vt1} and x_{vt2} are the turning points of the volume produced H^- ions for $x'_v < x_{min}$ and $x'_v > x_{min}$, respectively, and x_{min} is the position of the minimum potential, $E_{min} = q\phi(x)$ and $E_{min-} = -q\phi(x)$. By interchanging the order of integrations of Eqs. (7), (8), and (9), the ion densities are obtained as

$$n_i(x) = 2\int_0^L dx'_i \int_{q\varphi(x'_i)}^{\infty} dE_i \frac{1}{\upsilon_i(x,E_i)} \frac{S_i(x'_i,E_i)}{\upsilon_i(x'_i,E_i)}, \tag{13}$$

$$n_v(x) = 2\int_0^L dx'_v \int_{E_{v0}}^{\infty} dE_v \frac{1}{\upsilon_v(x,E_v)} \frac{S_v(x'_v,E_v)}{\upsilon_v(x'_v,E_v)}, \tag{14}$$

$$n_s(x) = 2\int_0^L dx'_s \int_{-q\phi_{min}}^{\infty} dE_s \frac{1}{\upsilon_s(x,E_s)} \frac{S_s(x'_s,E_s)}{\upsilon_s(x'_s,E_s)} + 2\int_{x_{min}}^L dx'_s \int_{-q\phi(x)}^{-q\phi_{min}} dE_s \frac{1}{\upsilon_s(x,E_s)} \frac{S_s(x'_s,E_s)}{\upsilon_s(x'_s,E_s)}, \tag{15}$$

where $E_{v0} = \max\{-q\phi(x), -q\phi(x'_v)\}$. As the source function we use the expression same as the Emmert *et al*. [8]

$$S_i(x,E_i) = \frac{S_{i0}h_i(x)}{2kT_i} \exp\left\{-\frac{E_i - q\phi(x)}{kT_i}\right\}, \tag{16}$$

$$S_v(x,E_v) = \frac{S_{v0}h_v(x)}{2kT_v} \exp\left\{-\frac{E_v + q\phi(x)}{kT_v}\right\}, \tag{17}$$

$$S_s(x,E_s) = \frac{S_{s0}h_s(x)}{2kT_s} \exp\left\{-\frac{E_s + q\phi(x)}{kT_s}\right\}, \tag{18}$$

where k is the Boltzmann's constant, T_i, T_v, and T_s are the temperatures, $h_i(x)$, $h_v(x)$, and $h_s(x)$ are the source strengths, and S_{i0}, S_{v0}, and S_{s0} are the average source strengths. The averages about x of $h_i(x)$, $h_v(x)$, and $h_s(x)$ are normalized to 1. By substituting Eqs. (16), (17), and (18) to Eqs. (13), (14), and (15) and integrating them for E_i, E_v, and E_s, we obtain

$$n_i(x) = \left(\frac{M_i\pi}{2kT_i}\right)^{1/2} S_{i0}\int_0^L dx'_i I_i(x,x'_i)h_i(x'_i), \tag{19}$$

$$n_v(x) = \left(\frac{M_v\pi}{2kT_v}\right)^{1/2} S_{v0}\int_0^L dx'_v I_v(x,x'_v)h_v(x'_v), \tag{20}$$

$$n_s(x) = \left(\frac{M_s\pi}{2kT_s}\right)^{1/2} S_{s0}I_s(x,L)h_s(L), \tag{21}$$

where $h_s(x'_s) = h_s(L)$ due to the surface produced H^- ions are produced only on the wall surface, and

$$I_i(x,x'_i) = \begin{cases} \exp\left\{\dfrac{q\phi(x'_i) - q\phi(x)}{kT_i}\right\} \cdot \operatorname{erfc}\left[\left\{\dfrac{q\phi(x'_i) - q\phi(x)}{kT_i}\right\}^{1/2}\right], & q\phi(x'_i) > q\phi(x), \\ \exp\left\{\dfrac{q\phi(x'_i) - q\phi(x)}{kT_i}\right\}, & q\phi(x'_i) < q\phi(x), \end{cases} \tag{22}$$

$$I_v(x,x'_v) = \begin{cases} \exp\left\{\dfrac{-q\phi(x'_v) + q\phi(x)}{kT_v}\right\} \cdot \operatorname{erfc}\left[\left\{\dfrac{-q\phi(x'_v) + q\phi(x)}{kT_v}\right\}^{1/2}\right], & q\phi(x'_v) < q\phi(x), \\ \exp\left\{\dfrac{-q\phi(x'_v) + q\phi(x)}{kT_v}\right\}, & q\phi(x'_v) > q\phi(x), \end{cases} \tag{23}$$

$$I_s(x,L) = \begin{cases} \exp\left\{\dfrac{-q\phi(L) + q\phi(x)}{kT_s}\right\} \cdot \operatorname{erfc}\left[\left\{\dfrac{-q\phi_{min} + q\phi(x)}{kT_s}\right\}^{1/2}\right], & x < x_{min} \\ \exp\left\{\dfrac{-q\phi(L) + q\phi(x)}{kT_s}\right\}, & x > x_{min}, \end{cases} \tag{24}$$

where $\operatorname{erfc}(x)$ is the complementary error function. For the electron density, we use a Boltzmann distribution

$$n_e(x) = n_0 \exp[e\phi(x)/kT_e], \tag{25}$$

for simplicity, where n_0 is the electron density at $x = 0$, $-e$ is the electron charge, and T_e is the electron temperature. Substituting Eqs. (19), (20), (21) and (25) into Poisson's equation, the plasma-sheath equation is derived

$$\frac{d^2\phi(x)}{dx^2} = \frac{n_0 e}{\varepsilon_0}\exp\left(\frac{e\phi(x)}{kT_e}\right) - \frac{S_{i0}q}{\varepsilon_0}\left(\frac{M_i\pi}{2kT_i}\right)^{1/2} \cdot \int_0^L dx'_i I_i(x,x'_i)h_i(x'_i) + \frac{S_{v0}q}{\varepsilon_0}\left(\frac{M_v\pi}{2kT_v}\right)^{1/2}\int_0^L dx'_v I_v(x,x'_v)h_v(x'_v) + \frac{S_{s0}q}{\varepsilon_0}\left(\frac{M_s\pi}{2kT_s}\right)^{1/2} I_s(x,L)h_s(L). \tag{26}$$

The average source strengths S_{i0}, S_{v0} and S_{s0} are determined by the equilibrium of the fluxes of the plasma particles at the wall, that is, $j_{ew} + j_{iw} + j_{vw} - j_{sw} = 0$ and by defining the production rate of the volume produced H^- ion to be $\beta_v = S_{v0}/S_{i0}$ and that of the surface produced H^- ion to be $\beta_s = S_{s0}/S_{i0}$. Where j_{ew}, j_{iw}, j_{vw}, and j_{sw} are the current densities at the wall, and $j_{ew} = -en_0[kT_e/(2\pi m_e)]^{1/2}\exp[e\phi_w/(kT_e)]$ from $j_e = (1/4)n_e e\langle\upsilon_e\rangle$, $\langle\upsilon_e\rangle = [8kT_e/(\pi m_e)]^{1/2}$ and Eq. (25), $j_{iw} = qS_{i0}L$ from $\nabla\cdot j_i = qS(x)$, $j_{vw} = -qS_{v0}L$, $j_{sw} = -qS_{s0}L$, and ϕ_w is the wall potential.

$$S_{i0} = \frac{en_0}{qL(1+\beta_s-\beta_v)}\left(\frac{kT_e}{2\pi m_e}\right)^{1/2}\exp\left(\frac{e\phi_w}{kT_e}\right), \tag{27}$$

$$S_{v0} = \frac{\beta_v en_0}{qL(1+\beta_s-\beta_v)}\left(\frac{kT_e}{2\pi m_e}\right)^{1/2}\exp\left(\frac{e\phi_w}{kT_e}\right), \tag{28}$$

$$S_{s0} = \frac{\beta_s e n_0}{qL(1+\beta_s-\beta_v)}\left(\frac{kT_e}{2\pi m_e}\right)^{1/2}\exp\left(\frac{e\phi_w}{kT_e}\right). \quad (29)$$

3. Numerical Solutions

Since Eq. (26) cannot be solved analytically, it is solved numerically. We introduce the normalized variables such as $\eta = (q/kT_e)(\phi_w - \phi)$, $s = x/L$, $s' = x'/L$, $s'_v = x'_v/L$, $s'_s = x'_s/L$, $\tau_i = T_e/T_i$, $\tau_v = T_e/T_v$, $\tau_s = T_e/T_s$, and $Z = q/e$, where $Z = 1$ for the hydrogen plasma. The boundary conditions are $d\eta/ds|_{s=0} = 0$ and $\eta(s = 1) = 0$. The profile of the normalized electric potential $\Phi(s) = -\eta$ for various values of the production amount of the volume produced H^- ion to the H^+ ion is shown in Fig. 3, where $\tau = 2$, $\tau_s = 5$, $\tau_v = 2.5$, $\beta_s = 0.4$, and $\lambda_D/L = 5 \times 10^{-2}$, where λ_D is the Debye length. We will use the value of $\lambda_D/L = 5\times10^{-2}$ in all results of this paper. Although the effect of the volume produced H^- ion is not large, as the production rate β_v increases, the electric potential difference between the PG and the inside decreases. It seems that this is because the electrons toward the PG surface decrease due to the volume produced H^- ions, as a result, the potential drop decreases. The profile of the normalized electric potential for various values of the production amount of the surface produced H^- ion to the H^+ ion is shown in Fig. 4, where $\beta_v = 0.2$ and the values of τ, τ_s, and τ_v are same with Fig. 3. The electric potential is qualitatively almost the same as that without the volume produced H^- ions [9], that is, as the production rate β_s increases a negative peak is appeared near the PG surface, although the electric potential is a little low due to the volume produced H^- ions.

The density distributions of the plasma particles are derived from Eqs. (19), (20), (21), (25) and the electric potential. The profile of the plasma density normalized by a sum of the H^+ ion density and the H^- ion density at $s = 0$, that is, $n_i(0) + n_v(0) + n_s(0)$, for cases of $\beta_v = 0$, 0.1, 0.2, and 0.3 is shown in Fig. 5, where other parameters are same with Fig. 3. It is shown that the plasma density strongly depends on the production rate of the volume produced H^- ion. As the value of β_v increases, the density of other particles decreases, especially the electron density. As a result, the region consisting of the H^+ ions and the H^- ions more than the electrons appears near the extraction region. The profile of the normalized plasma density for cases of $\beta_s = 0$, 0.2, 0.4, and 0.6 is shown in Fig. 6, where other parameters are same with Fig. 4. The effect of the production rate of the surface produced H^- ions on the particle density is qualitatively almost the same with that without the volume produced H^- ions [9], that is, as the value of β_s increases the double ion plasma layer is formed near the PG surface, although the electron density is low in whole of the extraction region due to the volume produced H^- ions, which is also found from comparison between Fig. 5 (a) and Fig. 6 (c).

The effects of the temperature of the volume produced H^- ion and the surface produced H^- ion on the electric potential distribution and the density distribution of other particles are small. In the case of the temperature of the volume produced H^- ion is low, that is, τ_v is large, the density of the volume produced H^- ion near the extraction region becomes large except for near the PG surface as shown in Fig. 7. It seems that this is because the low energy volume produced H^- ions are moved to interior of the ion source by the sheath potential. In the case of the temperature of the surface produced H^- ion is low, that is, τ_s is large, the density of the surface produced H^- ion near the PG surface becomes large as shown in Fig. 8. It seems that this is because the low energy surface produced H^- ions produced on PG surface are difficult to move and stay near the PG surface, as a result the density of the surface produced H^- ion becomes large near the PG surface.

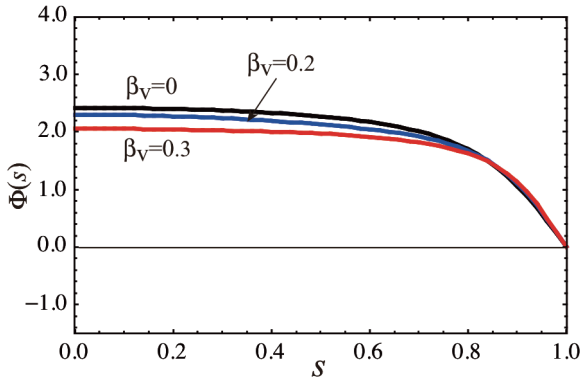

Fig. 3 Profile of the normalized electric potential for various values of β_v with $\tau = 2$, $\tau_v = 2.5$, $\tau_s = 5$, $\beta_s = 0.4$.

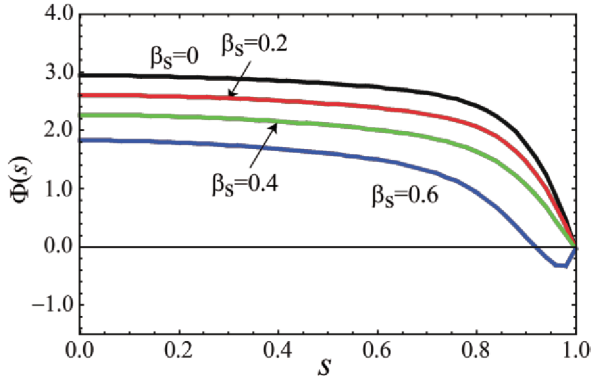

Fig. 4 Profile of the normalized electric potential for various values of β_s with $\tau = 2$, $\tau_v = 2.5$, $\tau_s = 5$, $\beta_v = 0.2$.

4. Conclusions

The distributions of the electric potential and the plasma density near the extraction region for the plasma considering the surface produced H^- ions and the volume produced H^- ions in addition to the electrons and the H^+ ions are studied analytically. The plasma-sheath equation is derived theoretically and solved numerically. As the production amount of the volume produced H^- ion increases,

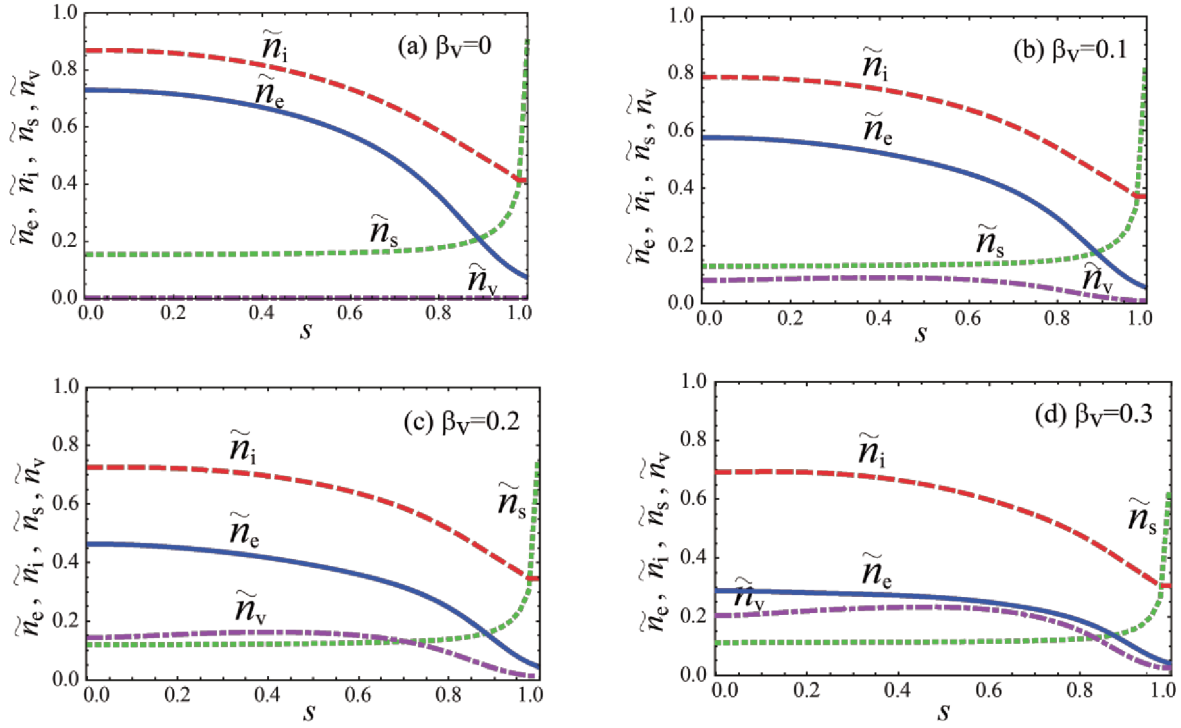

Fig. 5 Profile of the normalized plasma densitiy for various values of β_v, with $\tau = 2$, $\tau_v = 2.5$, $\tau_s = 5$, $\beta_s = 0.4$.

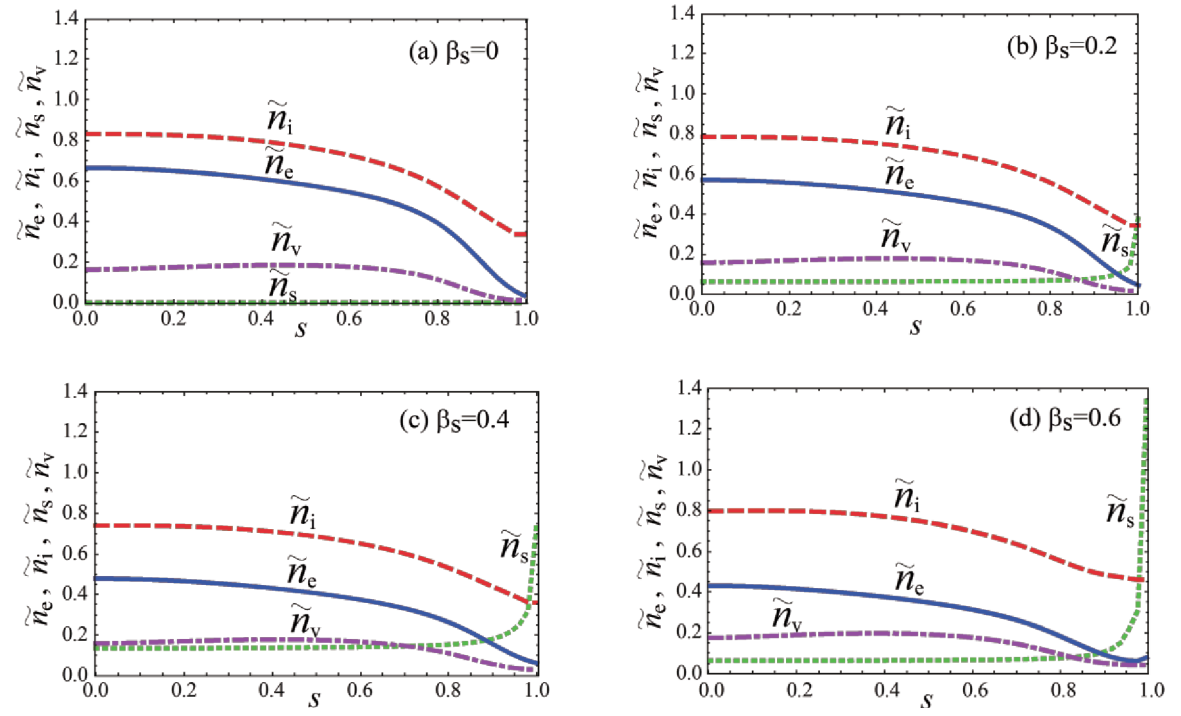

Fig. 6 Profile of the normalized plasma density for various values of β_s, with $\tau = 2$, $\tau_v = 2.5$, $\tau_s = 5$, $\beta_v = 0.2$.

the electron density is particularly decreased and the region where the H^+ ions and H^- ions exist more than the electrons appears near the extraction region. The effect of the surface produced H^- ions on the distributions of the electric potential and the plasma density is qualitatively almost same as the result for the case that the volume produced H^- ions are not considered. Although the effects of the temperature of the volume produced H^- ion and the surface produced H^- ion on the electric potential distribution and the density distribution of other particles are small, their density distributions depend on their temperature, respectively.

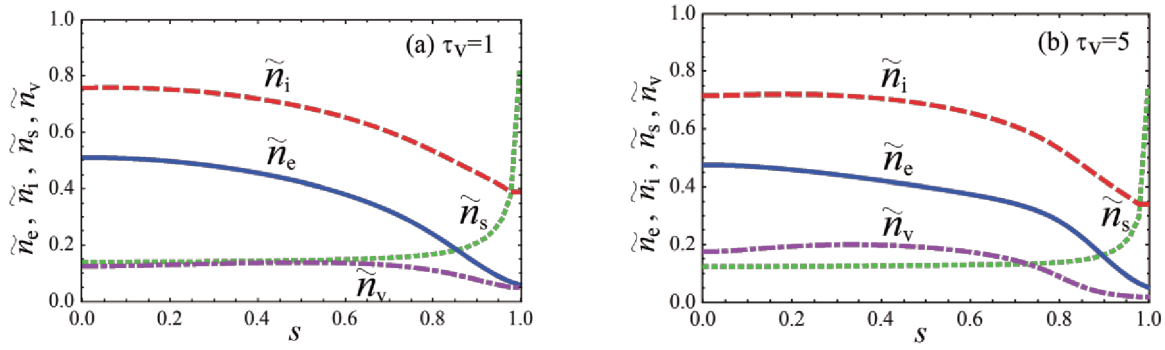

Fig. 7 Profile of the normalized plasma density for cases of (a) $\tau_v = 1$ and (b) $\tau_v = 5$, with $\tau = 2$, $\tau_s = 5$, $\beta_v = 0.2$, $\beta_s = 0.4$.

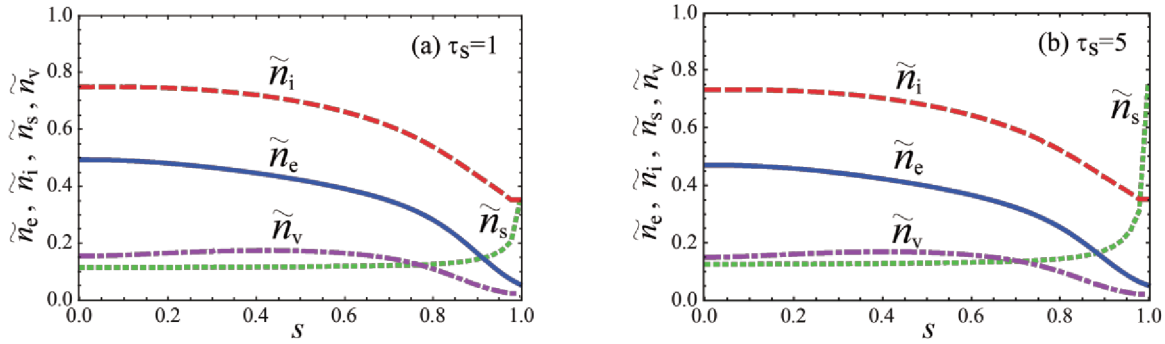

Fig. 8 Profile of the normalized plasma densities for case of (a) $\tau_s = 1$ and (b) $\tau_s = 5$, with $\tau = 2$, $\tau_v = 2.5$, $\beta_s = 0.4$, $\beta_v = 0.2$.

[1] H. Amemiya, B.M. Annaratone and J.E. Allen, J. Plasma Phys. **60**, 81 (1998).
[2] R. McAdams and M. Bacal, Plasma Source Sci. Technol. **19**, 042001 (2010).
[3] D. Wunderich, R. Gutser and U. Fantz, Plasma Source Sci. Technol. **18**, 045031 (2009).
[4] R. McAdams, A.J.T. Holmes, D.B. King and E. Surrey, Plasma Source Sci. Technol. **20**, 035023 (2011).
[5] F. Taccogna, P. Minelli, S. Longo, M. Capitelli and R. Schneider, Phys. Plasmas **17**, 063502 (2010).
[6] A. Hatayama, Rev. Sci. Instrum. **79**, 02B901 (2008).
[7] K. Tsumori, H. Nakano, M. Kisaki, K. Ikeda, K. Nagaoka *et al.*, Rev. Sci. Instrum. **83**, 02B116 (2012).
[8] G.A. Emmert, R.M. Wieland, A.T. Mense and J.N. Davidson, Phys. Fluids **23**, 803 (1980).
[9] A. Fukano and A. Hatayama, Rev. Sci. Instrum. **85**, 02B123 (2014).